14th International Symposium on Turbulence and Shear Flow Phenomena (TSFP14)
Heidelberg, Germany, July 28–31, 2026

NUMERICAL SIMULATION OF THE INTERACTION OF A SHOCK WAVE WITH A TURBULENT SHEAR LAYER USING HIGH ORDER SPECTRAL DIFFERENCE METHODS

Matthias Frey*, **Andrea Sanchez, Marc Montagnac, Romain Gojon, Jérémie Gressier and Stéphane Jamme**
ISAE-SUPAERO, University of Toulouse, France
*email: matthias.frey@isae-supaero.fr

ABSTRACT

This paper presents a numerical study of a spatially developing turbulent shear layer and its interaction with an oblique shock wave using a Spectral Difference (SD) method. The goal of this study is to evaluate the performance of different subgrid-scale models and shock capturing strategies for the high-order simulation of supersonic flows, that comprise both turbulence and strong discontinuities. In a first step, simulations were conducted for a pure shear layer to compare a subgrid-scale model that is particularly adapted for SD methods to classical approaches. In the next step, an impinging oblique shock wave has been added to the configuration and a new artificial viscosity-based shock capturing method has been compared to a slope limiter based on a local reduction of the polynomial order of the numerical scheme. The influence of the shock capturing scheme on the spatially developing turbulence has been measured and compared to a reference solution obtained with a refined mesh.

INTRODUCTION

Efficient computation of turbulent supersonic flows plays a key role in the design of supersonic as well as transsonic aircraft. Flow configurations comprising strong normal and oblique shock waves can be found in several regions of the vehicle, including the air inlet, the wings and the engine nozzles. In particular the interaction of shock waves with turbulent shear and boundary layers provokes shock oscillations that can cause phenomena such as wing buffeting or inlet buzz phenomena. This flow behavior entails strong pressure fluctuations, that have a harmful effect on the aircraft efficiency and structure integrity. To gain insight into the physical effects that are driving these phenomena, a scale resolving numerical approach is required to capture the dynamics of turbulent structures. Large Eddy Simulations (LES) provide an adequate tool to gain satisfactory insights into the intricacies of the dynamic flow phenomena at a bearable cost.

However, the combined presence of a large variety of scales and strong gradients require a robust and accurate code to perform simulations of supersonic configurations. Due to their high precision and convergence rate, high-order methods like Discontinuous Galerkin (DG) or Spectral Difference (SD) methods have gained strong interest in the past years for the simulation of such complex flow configurations. In particular, their robustness for non-regular unstructured meshes, their high ability for efficient parallelization and the considerably easier mesh generation and handling makes high-order approaches promising methods to gradually replace the classical Finite Volume method in the future. For the successful application of these methods on complex supersonic flows, two key ingredients are required: a robust subgrid-scale model has to detect regions in the flow, where the physical dissipation is impaired due to the lack of resolved dissipative scales and has to add artificial dissipation in order to maintain a proper energy balance of the flow. Secondly, the polynomial interpolation applied in high-order methods is prone to the appearance of Gibbs oscillations if the solution comprises sharp gradients or discontinuities such as strong shock waves. These oscillations pollute the physics of the flow and can even destabilize the solver and eventually provoke a simulation breakdown. To deal with this issue, a shock capturing mechanism has to detect the affected cells and locally apply a stabilization scheme in order to mitigate the detrimental effect of the oscillations.

While several subgrid-scale models and shock capturing strategies have been proposed in the past years, their performance for high-order spectral methods applied on complex flow configurations has not been clearly evaluated yet. In particular, the ability of the methods to restrict their dissipative behavior to the locally required quantity has to be proved. Suboptimally defined or badly calibrated mechanisms may fulfill their primary task to stabilize the flow but exhibit undesired behavior elsewhere and alter the flow physics in an unacceptable manner. This effect can arise from a poor detection of the affected cells that require the numerical treatment or from the methodology and intensity of the treatment method itself.

In order to gain more insight on the subject, this paper investigates the performance of recently proposed strategies for subgrid-scale modeling and shock capturing, that are particularly adapted for high-order methods. This study aims to provide a numerical validation of these methods to enable their application on complex supersonic flows for actual aerospace applications. For this numerical validation, a test case has been chosen, that consists of the interaction of an oblique shock wave with a spatially developing turbulent mixing layer. This case aims at studying the behavior of both ingredients on an essentially three-dimensional and fully turbulent flow configuration at a very moderate meshing effort and numerical cost. Even though, this paper focuses on the Spectral Difference (SD) method, the results obtained in this investigation can be adapted for any high-order method, that is based on polynomial interpolation.

METHODOLOGY

In this section, at first the numerical model is described with an emphasis on the applied shock capturing and subgrid-scale modeling strategies. Then, the physical definition of the chosen shear layer configuration is presented.

Numerical model

The numerical simulations were performed with the inhouse solver IC^3 by solving the compressible Navier Stokes equations on an unstructured hexahedral grid. For spatial discretization, the Spectral Difference (SD) method introduced by Wang (2002) has been applied. This high-order method is based on a subdiscretization of the mesh elements into a set of solution points and flux points. Inside each cell, the numerical solution may be obtained by a polynomial interpolation of order p in each spatial direction. To obtain the numerical fluxes, this solution is extrapolated on the element flux points of order $p+1$. The fluxes are then exchanged with the adjacent elements at the shared face point and re-interpolated on the solution points. During the flux exchange, discontinuities between two neighboring cells are treated by a HLLC Riemann solver. This method provides a robust high-order scheme, that allows compact implementation and efficient parallelization. Throughout this numerical study, a spectral scheme of a constant polynomial order of four has been applied. For temporal advancement of the simulation, an explicit three-stage Runge-Kutta scheme has been used.

In order to provide sufficient dissipation for the under-resolved simulation of the turbulent mixing layer, three different subgrid-scale modeling approaches have been tested. The study focused hereby in particular on the comparison of the recently proposed Spectral Element Dynamic Model (SEDM) presented by Chapelier & Lodato (2016) to established models like the Vreman model presented by Vreman (2004) and the SIGMA model presented by Nicoud *et al.* (2011). While the static Vreman and SIGMA models have been originally proposed for Finite Volume solvers, the SEDM model has been developed specifically for the high-order Spectral Difference scheme. Hereby the SEDM model takes advantage of the polynomial interpolation and dynamically measures the degree of under-resolution via a modal decomposition of the interpolated solution. This methodology allows a proper detection of flow regions that require additional dissipation. Since the SEDM model has been proposed recently, a proper validation on transitional shear flows has not been provided yet.

In order to deal with Gibbs oscillations among the shock wave and to stabilize the high-order solver, two different shock capturing strategies have been tested. This study hereby focused on the comparison of the mitigation of the oscillation intensity via a slope limiter and the dissipation of the oscillations via the local application of artificial dissipation. As slope limitation method, the Spatially Weighted Projection (SWeP) limiter presented by Lamouroux *et al.* (2016) has been applied which is based on conducting a weighted interpolation of the solution function using a polynomial of lower order. For the second approach, the physical artificial viscosity-based method proposed by Fernandez *et al.* (2018) was used. This method applies artificial bulk viscosity to the viscous fluxes of the Navier-Stokes equations. For the detection of the mesh elements, in which a shock capturing treatment is required, the modal shock sensor presented by Persson & Peraire (2006) was applied in both approaches. Analogous to the resolution sensor used by the SEDM subgrid-scale model, this sensor detects sharp gradients by evaluating the exponential decay of the modal interpolation coefficients. The amount of applied artificial dissipation is then chosen via a continuous activation function. Both shock capturing strategies add a certain amount of non-physical dissipation, which has a physical impact on the flow. In particular, the similarity of turbulence and shock waves concerning local gradients poses a challenge to restrict the amount of dissipation to purely shock-dominated regions. Studying the impact of these artificial mechanisms on the flow and in particular on the integrity of turbulent structures is the main goal of this study.

Physical configuration

The physical characteristics of the spatially evolving shear layer were chosen based on the numerical work provided by Pantano & Sarkar (2002) using a convective Mach number $M_c = \frac{U_1-U_2}{c_1+c_2}$ of 0.3. The applied inflow conditions of the turbulent mixing layer are presented in table 1.

Table 1: Flow parameters of the shear layer

Flow parameter	Top flow	Bottom flow
M_1, M_2	1.91	1.36
U_1, U_2 $[m/s]$	575	399
P $[Pa]$	$49 \cdot 10^5$	$49 \cdot 10^5$

For a smooth transition between the two flow regimes in the initial state and at the inlet, a hyperbolic-tangent velocity profile described in equation (1) has been imposed:

$$u_x(y) = \frac{U_1+U_2}{2} + \frac{U_2-U_1}{2} \tanh\left(\frac{2y}{\delta_{\omega,0}}\right) \qquad (1)$$

Here $\delta_{\omega,0}$ denotes the vorticity thickness at the inflow, that is defined as $\delta_\omega = \Delta U/\max(\partial U/\partial y)$. The initial vorticity thickness $\delta_{\omega,0}$ was chosen based on the Reynolds number $Re_\omega = \frac{u\,\delta_\omega}{\nu}$ of 640, that was used in the work of Pantano & Sarkar (2002).

The numerical domain size was chosen as $0 \leq$ x ≤ 0.3 m, -0.024 $\leq$ y $\leq$ 0.024 m and $0 \leq$ z ≤ 0.02 m with x denoting the mean flow direction and z the transverse direction. In order to trigger the formation of Kelvin-Helmholtz instabilities the method presented by Bogey *et al.* (2012) has been applied. This approach promotes the excitation of instabilities by locally adding periodic perturbations in the horizontal and vertical inflow components. The perturbations are imposed with a harmonic pulsation of the frequency

$$f = 0.132\;(U_c/\delta_{\omega,0}), \qquad (2)$$

where $U_c = (U_1+U_2)/2$ denotes the convection velocity of the mixing layer. This frequency corresponds to the most effective mode to trigger instabilities in a hyperbolic-tangent velocity profile following the linear stability theory of Michalke (1964). To excite a destabilization in spanwise direction, the hyperbolic-tangent velocity profile was furthermore coupled with an arbitrary periodic modulation in transverse direction, which provoked a gradual transition from the fully laminar inflow to a three-dimensional turbulent mixing layer.

Separate simulations were performed of the pure turbulent shear layer and of the shear layer with shock wave interaction.

Periodic boundary conditions were chosen in the spanwise direction while a symmetry condition was imposed at the bottom of the domain to avoid the development of a boundary layer. For the simulations of a pure shear layer, a symmetry condition was applied at the domain top as well. For the simulations of the shock wave-shear layer interaction, an oblique shock wave was added downstream of the transition region. In order to generate the shock wave, the top boundary condition was partially changed from the symmetry condition to a supersonic inflow. The inflow was imposed with a horizontal and a vertical component following the Rankine-Hugoniot relations to provoke the formation of an oblique shock wave with a deflection angle of 33 degrees. The shock wave is then reflected at the bottom of the domain which results in a second interaction with the shear layer further downstream.

RESULTS

The numerical results that are presented in this paper are split in two parts. First, the simulation of a pure shear layer is conducted in order to evaluate the performance of the sub-grid scale modeling strategies. Then, simulations of a shock wave-shear layer interaction are conducted with a focus on the performance of the shock capturing methods. A two-dimensional grid refinement study had been conducted first in order to tune the simulation parameters. Then, the chosen configuration was extruded in spanwise direction to obtain a three-dimensional domain. A data acquisition phase of more than ten convective cycles has been conducted after each transient initialization to obtain a proper representation of turbulence statistics.

Pure shear layer

A simulation of the pure shear layer is conducted without subgrid-scale model. For all simulations the domain is equally discretized using 600 x 180 x 40 degrees of freedom in the three spatial directions. A temporal vorticity snapshot is depicted in figure 8, that reveals three different flow regions. Right after the inlet, the flow is purely laminar and the mixing zone is restricted to the initial vorticity thickness. Then, a transition zone appears between around $100 \leq x/\delta_{\omega,0} \leq 200$ where an arising Kelvin-Helmholtz instability provokes the formation of two-dimensional vortex structures that rapidly turn into fully three-dimensional turbulence. With further spatial development downstream the thickness of the mixing zone is continuously increasing. Figure 1 depicts the spatial evolution of the vorticity thickness. As expected the figure reveals a linear growth which is a typical behavior for turbulent mixing layers. The first increase of the vorticity thickness at $x/\delta_{\omega,0} \approx 100$ marks the beginning of the transition phase.

The maximum value of the turbulent kinetic energy at every spatial location is depicted in figure 2. Again, the figure shows the beginning of the transition as turbulent kinetic energy begins to appear at $x/\delta_{\omega,0} \approx 100$. The figure then reveals that the turbulent kinetic energy does not continuously increase but reaches a peak value among $x/\delta_{\omega,0} \approx 220$ and slowly decreases further downstream. This effect arises due to the appearance of dissipative turbulent scales after the transition phase.

In the next step, simulations are performed using the three different subgrid-scale models: Vreman, SIGMA and SEDM, respectively. In figure 3 the normalized subgrid-scale viscosity along the shear layer centerline at y = 0 is depicted for the Vreman and the SIGMA model. The figure reveals that the desired behavior of applying zero viscosity inside the laminar region is fulfilled by both models. Both models begin to ac-

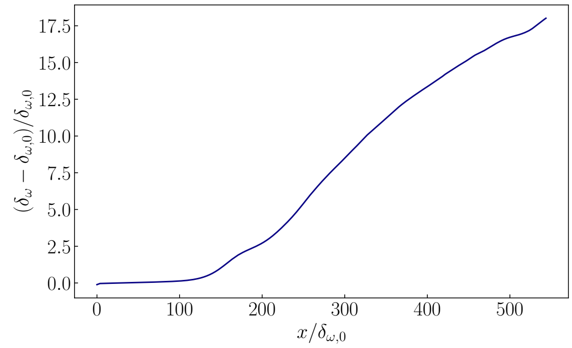

Figure 1: Spatial evolution of the vorticity thickness of the pure shear layer

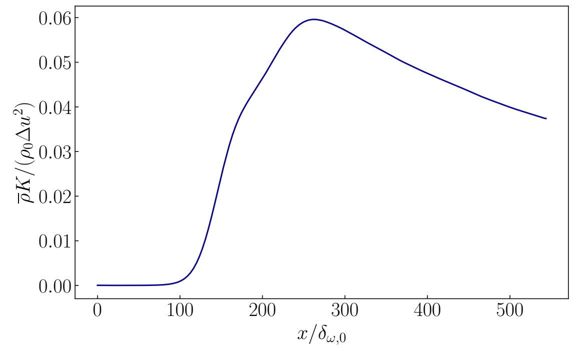

Figure 2: Spatial evolution of the maximum turbulent kinetic energy of the pure shear layer

tivate in the transition region, however the Vreman model is activated further upstream than the SIGMA model. Comparing the activation points of both models to the curves in figure 1 and 2 reveals that the SIGMA model correctly meets the inception of turbulence at $x/\delta_{\omega,0} > 100$ while the Vreman model activates too early, already at $x/\delta_{\omega,0} \approx 80$. A proper behavior of the subgrid-scale models in transitional regions is crucial since an excessive undesired activation can considerably alter the physics in this critical region and lead to wrong transition predictions. After the transition phase, both models reach a level of applied subgrid dissipation that stays constant along the developing shear layer further downstream. The results obtained with the SEDM model are shown in figure 4. The figure reveals, that the SEDM model does also apply zero viscosity in the laminar region. It is capable of detecting the transition region and it triggers the activation of the subgrid dissipation further downstream, where the transition to a fully turbulent flow is accomplished. The figure furthermore reveals, that the activation of the SEDM model reaches a peak value before it gradually decreases with further downstream development of the shear layer. Comparing this result to the maximum turbulent kinetic energy presented in figure 2, the SEDM model exhibits a similar behavior, while the Vreman and the SIGMA model do not follow the correct trend. A proper subgrid-scale model is expected to restrict and adapt its behavior to regions of intense and under-resolved turbulence. The results indicate that only the SEDM model exhibits this desired behavior while the Vreman and SIGMA models are not capable to adjust their intensity. This difference may result from the different model characteristics - while the Vreman and SIGMA models are static subgrid-scale models relying on local veloc-

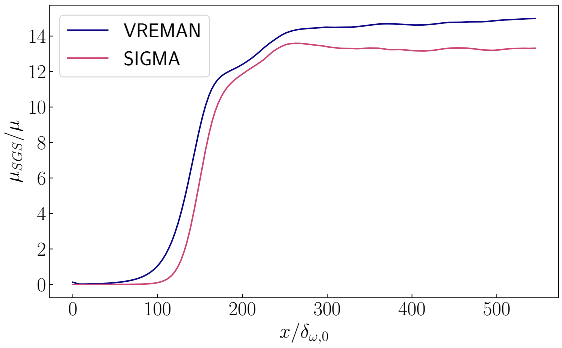

Figure 3: Spatial evolution of the subgrid-scale viscosity along the centerline using the static models Vreman and SIGMA

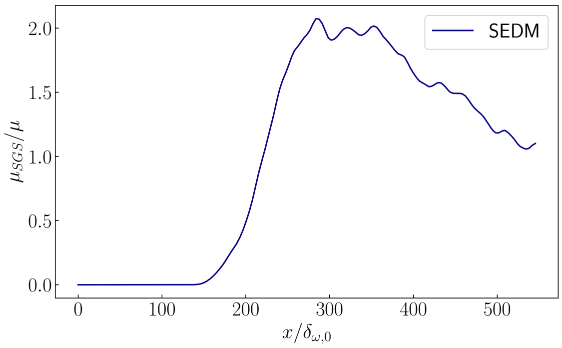

Figure 4: Spatial evolution of the subgrid-scale viscosity along the centerline using the dynamic SEDM model

ity gradients, the SEDM model relies on the quantification of the energy at the smallest resolved scales, in the same way as a dynamic model relies on a filtering operation. This strategy seems to give the best performance for the simulation of a turbulent mixing layer.

Shock wave-shear layer interaction

After the simulation of the pure shear layer, an oblique shock wave is added and the shock capturing mechanism is activated in order to stabilize the solver. These simulations were conducted without the application of any subgrid-scale model to purely study the dissipative effect of the shock capturing scheme. A temporal snapshot of the flow field is presented in figure 9.

Equal to the previous simulations the domain was discretized using 600 x 180 x 40 degrees of freedom in the three spatial directions. In order to provide a reference solution to compare with, one simulation was conducted without the use of a shock capturing scheme. To be able to conduct this simulation, the mesh was refined until a degree, where the amount of artificial dissipation, that is required to stabilize the high-order scheme, is small enough to permit the deactivation of the shock capturing mechanism. Three simulations were performed comparing the SWeP limiter and the physical artificial viscosity-based approach to the reference case. The influence of the discontinuity on the spatial development of the shear layer is presented in figure 5, which shows the spatial evolution of the vorticity thickness. The double interaction is clearly visible where the linear growth is sharply broken twice. Downstream of the impingement, the shear layer regains its linear growth rate. The figure reveals that while the results obtained using the physical artificial viscosity method correspond well to the reference results, the SWeP limiter exhibits a different behavior. In particular upstream of the shock interaction the growth rate differs from the reference solution. The figure shows that the transition phase and the evolution of a fully turbulent shear layer is significantly impeded by the activation of the SWeP limiter.

The spatial evolution of the maximum turbulent kinetic energy is depicted in figure 6. The figure reveals that the strong pressure gradient across the shock wave triggers a further generation of turbulent fluctuations. This leads to a slight increase of turbulent kinetic energy downstream of the interaction. Analogous to the vorticity thickness in figure 5, the figure reveals a significant difference between the reference results and the results obtained with the SWeP limiter, while the results obtained with the artificial viscosity method show a considerably better accordance. Note that an exact accordance is not realistic since the reference solution contains more resolved turbulent scales that exhibit a higher level of physical dissipation. However, the figures reveal a visibly lower quantity of turbulent kinetic energy present in the simulation using the SWeP limiter in comparison to the one using the physical artificial viscosity approach. This effect is particularly visible in the pure shear region upstream of the shock impingement.

To have a closer look at the turbulence intensity, the profiles of the Reynolds stresses are depicted in figure 7 at a spatial position of $x/\delta_{\omega,0} = 300$. The figure reveals that for each statistical quantity the values of the simulation using the SWeP limiter do not reach the level of the reference case. This effect is visible in particular for the vertical and spanwise velocity fluctuations. On the other hand, the values obtained with the artificial viscosity-based shock capturing scheme correspond more closely to the reference solution. These results indicate, that the amount of dissipation added by the SWeP limiter leads to a more excessive degradation of the turbulence inside the mixing layer. It is therefore responsible for a higher degree of pollution of the physics of the flow which leads to less satisfactory results for simulations of turbulent supersonic flows. On the other hand, the artificial viscosity shock capturing scheme seems to be able to stabilize the solver without severely altering the flow itself.

The activation of the shock capturing scheme inside purely turbulence-dominated regions and hence upstream of the interaction zone is caused by considerable pressure and density gradients inside the turbulent fluctuations, which are also detected by the modal shock sensor. Despite the existence of different enhancement approaches to restrict the sensor activation to purely shock-dominated regions, the dissipative stabilization mechanism will also affect turbulent structures. This highlights the necessity to construct a stabilization scheme that does not exhibit excessive damping of turbulent fluctuations.

Concerning the comparison of the computational efficiency of both shock capturing methods, the physical artificial viscosity method revealed a better performance as well. Indeed, for the same configuration with equal sensor parameters, the SWeP limiter required an about 10 percent higher computation cost. The higher values of preserved turbulent kinetic energy in comparison with the lower computational effort yield a strong indication to favor the artificial viscosity shock capturing method over the SWeP limiter for the simulation of highly turbulent supersonic flows.

An explication of the different performance can be driven from the formulation of the stabilization scheme itself: the

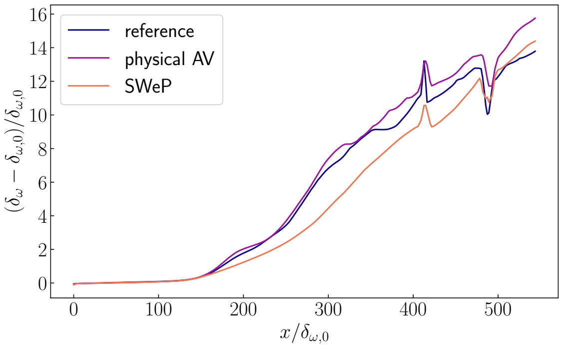

Figure 5: Spatial evolution of the vorticity thickness of the shock wave-shear layer interaction

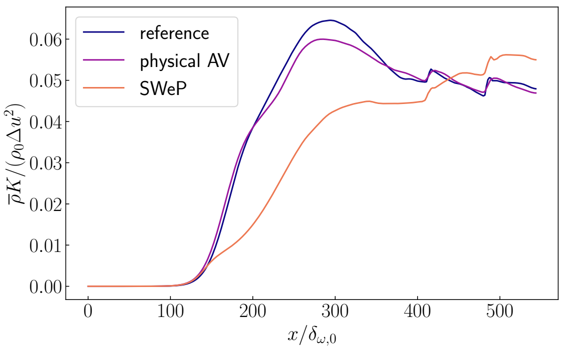

Figure 6: Spatial evolution of the maximum kinetic energy of the shock wave-shear layer interaction

SWeP limiter is based on a local reduction of the polynomial order inside the affected cell in combination with a spatially weighted projection of the solution. While this method can effectively remove the present Gibbs oscillations by limiting the slope of the interpolated function, it essentially comprises a local degradation of the order of accuracy. For the same flow structure, the solution is constructed via the projection of a reduced order polynomial, which yields a smearing effect on the vortices. This behavior is hence responsible for the degradation of the turbulence inside the spatially evolving shear layer and therefore the discrepancy with the reference result. The lower order interpolation and projection steps furthermore require additional matrix operations, that increase the computational effort required for the scheme.

On the other hand, the artificial viscosity method does not interfere with the numerical scheme and order of polynomial interpolation itself. Instead, it locally introduces a certain quantity of physical viscosity to the governing equations. This method preserves the same high-order of the interpolation polynomial throughout the whole domain. Since the stabilization is achieved without adding artificial shear viscosity μ, but through the application of bulk viscosity β only, the dissipative effect in shear direction is further reduced.

CONCLUSION

In this work, a spatially developing turbulent mixing layer and its interaction with an oblique shock wave has been investigated. In a first approach, simulations of a pure shear layer were conducted to evaluate the performance of different subgrid-scale models. The study revealed that all models stayed deactivated in the laminar zone, however only the SIGMA and SEDM model correctly detected the inception of the transition region while the Vreman model exhibited a too early activation. The results furthermore revealed that only the SEDM model was capable to detect the peak and decay zones of turbulent kinetic energy and to adapt its intensity.

Then, an oblique shock wave was added to compare the performance of two different shock capturing strategies to a reference solution obtained with a refined mesh. The results

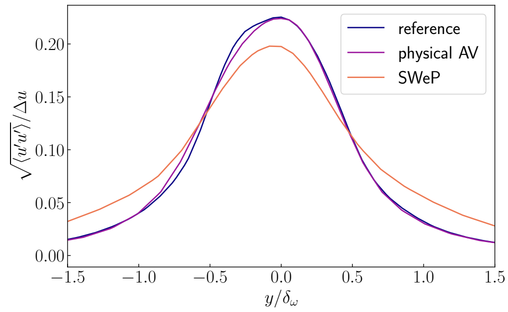

(a) $u'u'$

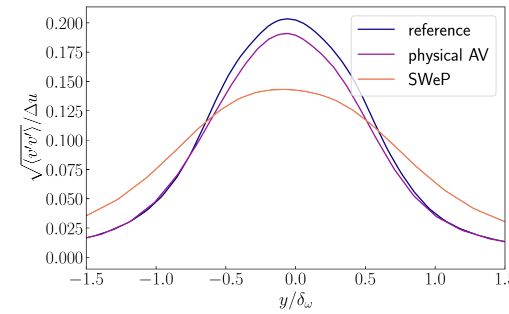

(b) $v'v'$

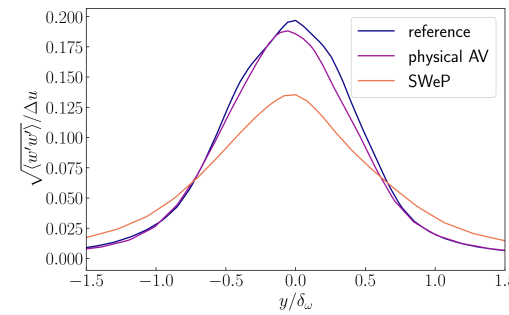

(c) $w'w'$

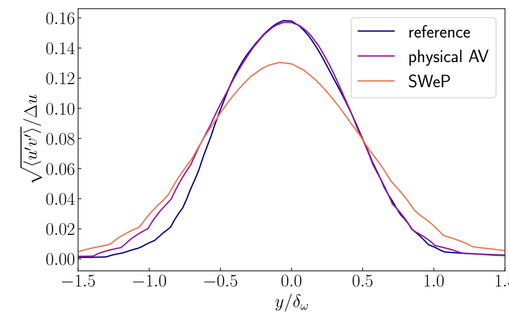

(d) $u'v'$

Figure 7: Comparison of turbulent statistics at a streamwise location of $x/\delta_{\omega,0} = 300$ of the shock wave-shear layer interaction

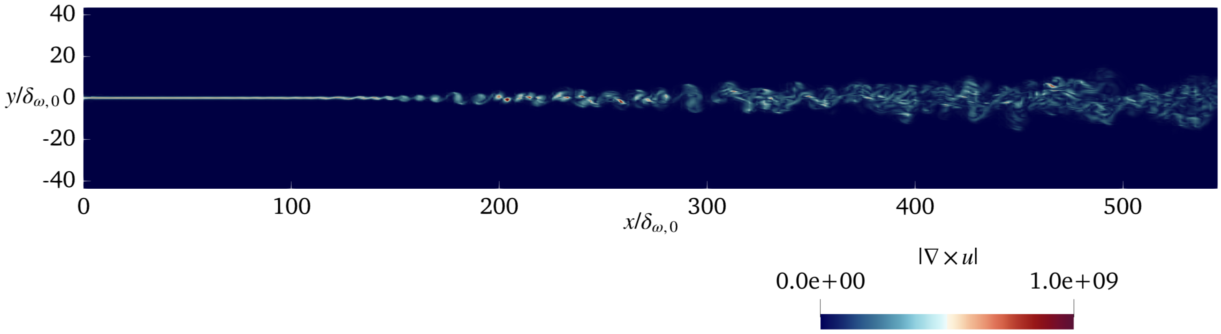

Figure 8: Instantaneous vorticity snapshot of the mixing layer revealing a transition region between $100 \leq x/\delta_{\omega,0} \leq 200$

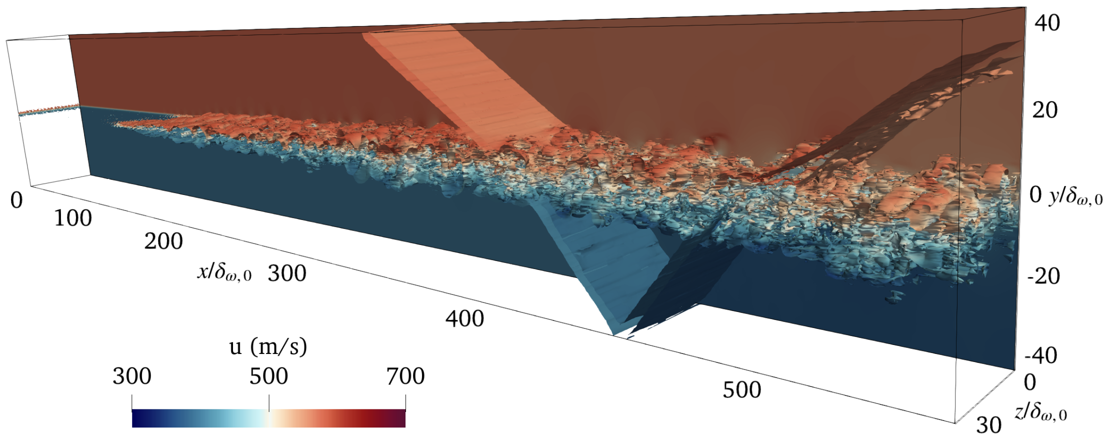

Figure 9: Instantaneous snapshot of the three-dimensional shock wave-shear layer interaction obtained with a fourth order spectral difference scheme. The shock wave and turbulent structures are highlighted via a contour of the pressure gradient

revealed that the SWeP limiter exhibited considerable dissipation of the shear layer beginning from the transition region. This effect leads to a different spatial evolution of the shear layer already upstream of the shock impingement. On the opposite, the results of the artificial viscosity based case correspond considerably better to the reference solution.

ACKNOWLEDGMENTS

This work was granted access to the HPC resources of CALMIP supercomputing center under the allocation 2025-P1425 as well as computing and storage resources by GENCI at TGCC thanks to the grant 2026-A0182A07178 on the supercomputer Joliot Curie's ROME partition.

REFERENCES

Bogey, C., Bailly, C. & Juve, D. 2012 Numerical simulation of sound generated by vortex pairing in a mixing layer. *AIAA Journal* **38** (12), 2210–2218.

Chapelier, J.-B. & Lodato, G. 2016 A spectral-element dynamic model for the large-eddy simulation of turbulent flows. *Journal of Computational Physics* **321**, 279–302.

Fernandez, P., Nguyen, C. & Peraire, J. 2018 A physics-based shock capturing method for unsteady laminar and turbulent flows. *2018 AIAA Aerospace Sciences Meeting* .

Lamouroux, R., Gressier, J. & Grondin, G. 2016 A high-order compact limiter based on spatially weighted projections for the spectral volume and the spectral differences method. *Journal of Scientific Computing* **67** (1), 375–403.

Michalke, A. 1964 On the inviscid instability of the hyperbolictangent velocity profile. *Journal of Fluid Mechanics* **19** (4), 543–556.

Nicoud, Franck, Toda, Hubert Baya, Cabrit, Olivier, Bose, Sanjeeb & Lee, Jungil 2011 Using singular values to build a subgrid-scale model for large eddy simulations. *Physics of Fluids* **23** (8), 085106.

Pantano, C. & Sarkar, S. 2002 A study of compressibility effects in the high-speed turbulent shear layer using direct simulation. *Journal of Fluid Mechanics* **451**, 329–371.

Persson, P.-O. & Peraire, J. 2006 Sub-cell shock capturing for discontinuous galerkin methods. *44th AIAA Aerospace Sciences Meeting and Exhibit* .

Vreman, A.W. 2004 An eddy-viscosity subgrid-scale model for turbulent shear flow: Algebraic theory and applications. *Physics of fluids* **16** (10), 3670–3681.

Wang, Z.J. 2002 Spectral (finite) volume method for conservation laws on unstructured grids. basic formulation: Basic formulation. *Journal of Computational Physics* **178** (1), 210–251.